AGU PUBLICATIONS

JGR

Journal of Geophysical Research: Earth Surface

RESEARCH ARTICLE

10.1002/2013JF002871

Key Points:
- Barrier island berm evolution is predictable
- Predictions depend on different storm climatologies and berm heights
- Results are applicable to a broad range of natural and restored features

Correspondence to:
N. G. Plant,
nplant@usgs.gov

Citation:
Plant, N. G., J. Flocks, H. F. Stockdon, J. W. Long, K. Guy, D. M. Thompson, J. M. Cormier, C. G. Smith, J. L. Miselis, and P. S. Dalyander (2014), Predictions of barrier island berm evolution in a time-varying storm climatology, *J. Geophys. Res. Earth Surf.*, *119*, doi:10.1002/2013JF002871.

Received 2 JUN 2013
Accepted 9 JAN 2014
Accepted article online 12 JAN 2014

Predictions of barrier island berm evolution in a time-varying storm climatology

Nathaniel G. Plant[1], James Flocks[1], Hilary F. Stockdon[1], Joseph W. Long[1], Kristy Guy[1], David M. Thompson[1], Jamie M. Cormier[1,2], Christopher G. Smith[1], Jennifer L. Miselis[1], and P. Soupy Dalyander[3]

[1]U.S. Geological Survey, Saint Petersburg Coastal and Marine Science Center, Saint Petersburg, Florida, USA, [2]Now at DigitalGlobe/GeoEye Inc., Tampa, Florida, USA, [3]U.S. Geological Survey, Woods Hole Coastal and Marine Science Center, Woods Hole, Massachusetts, USA

Abstract Low-lying barrier islands are ubiquitous features of the world's coastlines, and the processes responsible for their formation, maintenance, and destruction are related to the evolution of smaller, superimposed features including sand dunes, beach berms, and sandbars. The barrier island and its superimposed features interact with oceanographic forces (e.g., overwash) and exchange sediment with each other and other parts of the barrier island system. These interactions are modulated by changes in storminess. An opportunity to study these interactions resulted from the placement and subsequent evolution of a 2 m high sand berm constructed along the northern Chandeleur Islands, LA. We show that observed berm length evolution is well predicted by a model that was fit to the observations by estimating two parameters describing the rate of berm length change. The model evaluates the probability and duration of berm overwash to predict episodic berm erosion. A constant berm length change rate is also predicted that persists even when there is no overwash. The analysis is extended to a 16 year time series that includes both intraannual and interannual variability of overwash events. This analysis predicts that as many as 10 or as few as 1 day of overwash conditions would be expected each year. And an increase in berm elevation from 2 m to 3.5 m above mean sea level would reduce the expected frequency of overwash events from 4 to just 0.5 event-days per year. This approach can be applied to understanding barrier island and berm evolution at other locations using past and future storm climatologies.

1. Introduction

Low-lying coastal barrier islands are ubiquitous features around the world [*Price*, 1951] and the processes responsible for their formation, maintenance, and destruction have been described based on studies of the geologic record and from recent observations. Uncertainty in mechanisms for barrier island formation and maintenance is exacerbated by the variety of geologic and oceanographic settings that are capable of producing and supporting barrier islands [*Cattaneo and Steel*, 2003]. For example, barrier islands exist in a wide range of sea level rise [*Swift*, 1975], sea level fall [*Kroonenberg et al.*, 2000], and sediment supply [Stapor and Stone, 2004] scenarios. And, while barriers are defined by their persistent subaerial expression [*Price*, 1951], interactions of barriers islands with other features, such as dunes, berms, sand bars, and ebb tide deltas are important to barrier island evolution. Dunes and berms superimposed upon barrier islands contain sediment that can act to maintain the barrier's elevation and areal extent. And, the superimposed features form elevation perturbations that affect sediment transport processes via feedback between the morphology and the oceanographic processes [*Roelvink et al.*, 2009; *McCall et al.*, 2010]. For instance, interaction between dune height, beach width, and beach slope (among other morphologic variables) and different amounts of storm-induced runup leads to different types of barrier island evolution during storms [*Sallenger*, 2000; *Donnelly et al.*, 2006; *Stockdon et al.*, 2007; *Plant and Stockdon*, 2012].

Dune ridges and sandbars interacting with barriers can be found in environments with rapid sea level changes [*Thompson and Baedke*, 1995; *Kroonenberg et al.*, 2000], such as when ridges and bars are stranded as sea level falls. In a setting with net sediment accumulation, these barrier-building features can be preserved in the topographic and geologic record [*Tamura*, 2012]. Also, storms can trigger the

©2014. American Geophysical Union. All Rights Reserved.

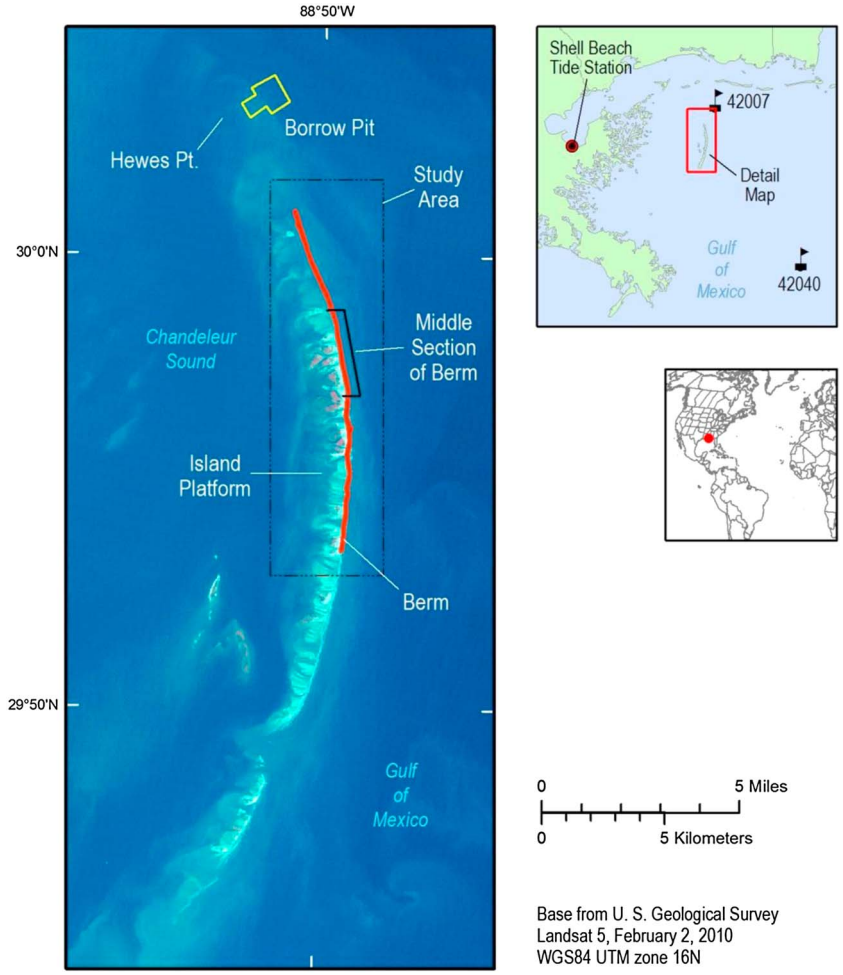

Figure 1. Chandeleur Islands study area.

formation or migration of bars that weld to the shore and interact with the overall barrier islands' sediment and elevation budgets [*Froede*, 2008]. Very commonly, barrier island perturbations such as dunes or berms are built by humans in order to reengineer the morphodynamic response of barriers by adding elevation to restrict wave overwash and, at the same time, altering the morphologic evolution of the barrier [*Jackson et al*., 2013]. These engineered perturbations can be so large or persistently maintained that natural barrier island overwash processes are altered for decades [*Schroeder et al*., 1977; *Riggs et al*., 2009]. Or, the perturbations can be relatively small such that overwash processes quickly alter the original design, serving as sediment additions that may be beneficial to the barrier maintenance [*Anderson et al*., 2010; *Van Den Hoek et al*., 2012; *Kelley*, 2013], but perhaps not necessarily ecologically optimal [*Saalfeld et al*., 2012; *Schupp et al*., 2013]. The Dutch "Zandmotor" is an example of an engineering experiment where a very large amount of sand (21.5 million m^3, or about twice the amount of sand used annually to nourish the Dutch coast) was added in front of a South Holland barrier beach in 2011 and was intended to interact with overwash and other processes as it continually feeds sand to adjacent beaches [*Van Den Hoek et al*., 2012].

The evolution of barrier islands is certainly tied to the evolution of large engineered or natural perturbations, such as high dunes. What is the role played by smaller perturbations, such as the engineered berms that are constructed to either add sand or borrow it from the barrier system and to alter the elevations in order to control the frequency of overwash? A part of the answer to this question can be obtained from models that can accurately predict the frequency of overwash, relate the overwash frequency to morphologic evolution, and then couple this predictive capability to knowledge of the

©2014. American Geophysical Union. All Rights Reserved.

oceanographic variability that drives overwash and other sediment transport processes. The resulting coupled modeling system can be used to evaluate expected rates of sediment dispersal and a return to preperturbation conditions of the modified barrier island system. And, with variable climate, sea level rise, and variations in storminess, a capability for making predictions of barrier island perturbation evolution can be used to identify the likelihood of alternative response scenarios of these features. Ultimately, this knowledge can be applied to understanding of overall barrier island response, including maintenance and possible destruction.

Modern engineering of barrier island berms for the purpose of barrier island maintenance and restoration combined with modern observing and modeling capabilities, offers an opportunity to improve our understanding of barrier island evolution. The "Zandmotor" in the Netherlands is one such example of this type of research that is underway. In response to the Deepwater Horizon oil spill in the Gulf of Mexico in 2010, a sand berm was constructed in front of and on the Chandeleur Islands (Figure 1). The berm's height was about 2 m above mean sea level, which was comparable to the height of low dunes present on the island prior to berm construction. The berm's construction and demise over the subsequent years provided an opportunity to identify mechanisms controlling berm evolution and to evaluate predictive models for describing this evolution and, ultimately, offers a chance to examine the interaction between the small perturbation of the berm with the larger barrier island. We have exploited this opportunity by focusing on understanding what aspects of this berm's evolution could be predicted through modeling and comparison to observations.

Our approach to this study was to develop and test a model that predicts changes in the linear extent of the berm based on predicted likelihoods of overwash events. We focused on the berm's linear extent because this information was readily available from frequent satellite imagery; other metrics such as berm width were not well resolved and berm height was sampled infrequently. And the linear extent metric included changes due to overwash processes, such as breaching, as well as changes at the terminal ends of the berm that might be driven by persistent alongshore transport gradients. The model includes terms that capture both episodic response (e.g., overwash events) and persistent response (e.g., due to alongshore-transport gradients). Once the model was fit to the data and its predictive skill was evaluated, it was used to examine the sensitivity of berm response to variations in storminess from a 16 year time series of oceanographic observations. In section 2 we provide some background on the Chandeleur Island evolution and berm construction history. Section 3 presents the morphological, oceanographic, and meteorological data and models used to describe and predict berm evolution. Section 4 presents an evaluation of intermediary oceanographic predictions required to predict overwash against a limited set of observations in order to assess hindcast and forecast accuracy of this component of the modeling system. Then, the berm evolution model, driven with the oceanographic predictions, was fit to the observed berm length changes in a hindcast comparison. Finally, in section 5, we present the results of a comparison of berm evolution predictions under alternative oceanographic climatologies that were drawn from the previous decade's observations. And we extend the model to a more generalized set of scenarios of berm evolution sensitivity to variations in berm elevation. Section 6 summarizes our primary findings that the timing of the observed berm evolution was predictable based, primarily, on the initial berm elevation and knowledge of storm climatology, and that the modeling approach can be used to understand generalized barrier island evolution scenarios.

2. Study Site

2.1. The History of the Chandeleur Islands

The Chandeleur Islands comprise a 30 km long chain of small islands located approximately 40 km east of the Mississippi River Delta separating the Gulf of Mexico from Breton Sound (Figure 1). The islands are described as a transgressive submergence barrier island system [*Penland et al.*, 1988], formed from the reworked deposits of the St. Bernard delta, a former delta complex of the Mississippi River. Distributaries of the former delta are preserved in the subsurface and are on average 3 m below the seafloor. These sediment-filled fluvial channels comprise an average 53% sand, 38% silt, and 9% clay, although some areas can contain up to 97% sand [*Flocks et al.*, 2009; *Twichell et al.*, 2009].

©2014. American Geophysical Union. All Rights Reserved.

Figure 2. Construction of the Chandeleur Islands' berm (USGS Photo taken 22 January 2011).

Sand within the buried channels was eroded, remobilized and deposited as barrier islands around an eroding headland, forming the platform for the island chain. At present, the islands are eroding rapidly due to diminished sediment supply, storm processes, and rapid relative sea level rise [*Suter et al*., 1988]. For example, between 1922 and 2004, the shoreline of the northern Chandeleur Islands was retreating at an average rate of between 12 and 38.4 m/yr [*Fearnley et al*., 2009]. Large storms after this period (e.g., Hurricanes Ivan in 2004 and Katrina in 2005) drove retreat rates of 200 m/yr [*Fearnley et al*., 2009].

Bathymetric change analysis shows that over the past century (1870 s–2006), approximately 285×10^6 m^3 of material, including both sand-sized and other finer sediment, has been eroded from the Chandeleur Island shoreface, of which 29% has been deposited in the back-barrier environment due to overwash events, and 45% has been transported to the north due to alongshore transport [*Miner et al*., 2009]. The material transported north and deposited at the terminal spit at Hewes Point (about $1x10^6$ m^3 yr^{-1}) has resulted in 8–10 m of vertical accretion. The Hewes Point sediment accounts for 36% of the material remaining along the entire Chandeleur Island platform [*Miner et al*., 2009; *Twichell et al*., 2009]. The sand deposit at Hewes Point is one of the largest in the muddy Mississippi River Delta Plain and a unique potential resource for shoreline restoration projects, or berm construction. Using numerical simulations of fair-weather conditions, *Ellis and Stone* [2006] identified a bimodal sediment transport system along the shoreface of the islands, with net transport northward along the northern two thirds of the island chain, and southward along the southern third. They estimated sediment transport rates of 63,000 m^3/yr to the north and 87,000 m^3/yr to the south, which is considerably slower than the historical rate based on observed deposition.

2.2. The Berm: Design, Construction, and Evolution

On 20 April 2010, the drilling rig *Deepwater Horizon* exploded approximately 130 km southeast of the Chandeleur Islands. Within 2 weeks, oil from the MC252 well leak was observed at the islands and elsewhere along the Louisiana coastline [*National Aeronautics and Space Administration*, 2010]. In May 2010, in an attempt to protect coastal wetlands, the State of Louisiana requested emergency authorization from the U.S. Army Corps of Engineers to construct sand berms along the coast to block the movement of oil. At Breton National Wildlife Refuge, the original plan called for the construction of three berm sections seaward of the islands starting just north of Hewes Point and extending 48 km south to the Mississippi River Delta [*Louisiana Department of Natural Resources*, 2010].

©2014. American Geophysical Union. All Rights Reserved.

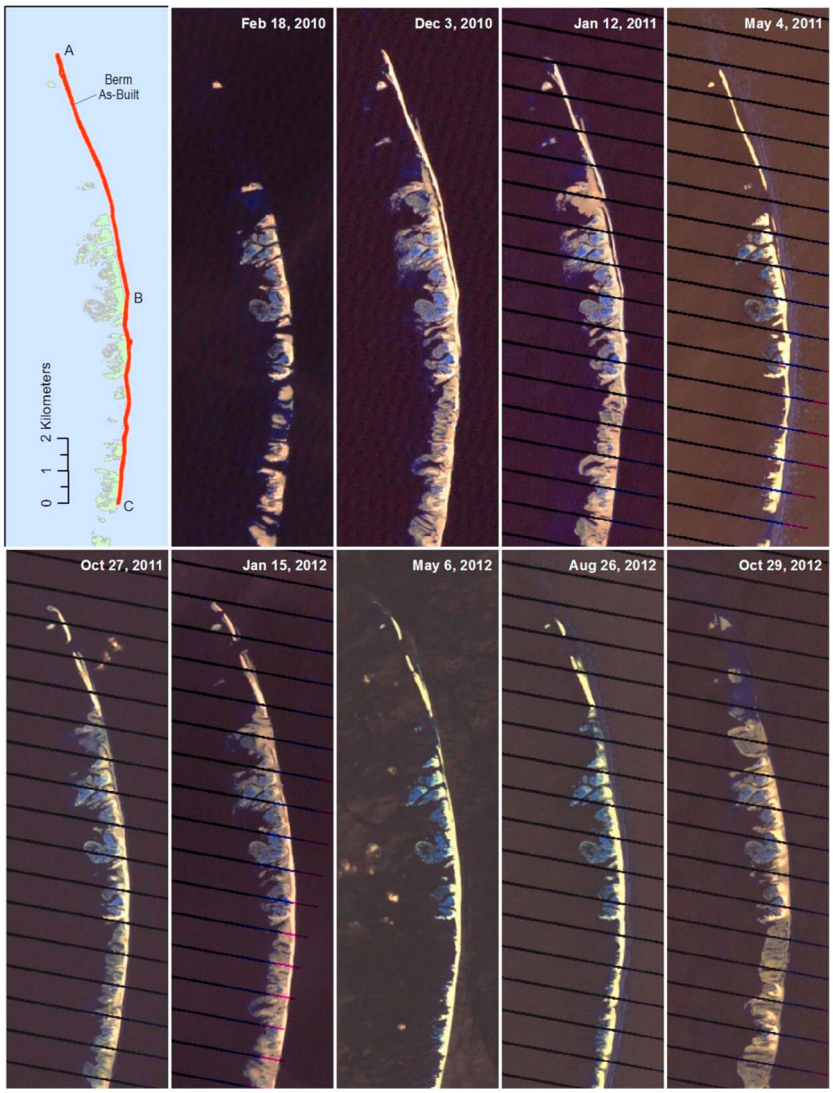

Figure 3. Construction and degradation of the E4 berm along the Chandeleur Islands from (a) north of the existing island fragments, along the submerged island platform to (b) in front of the island, and (c) on the island shoreface. The panel dated 18 February 2010 represents the natural island prior to berm construction.

The original plan was to build a sand berm that was 182 m wide at the base, 8 m wide at the top, 1.8 m (above mean sea level) high at its apex, with a 25:1 slope [*Louisiana Department of Natural Resources*, 2010]. The design-height was based on a requirement to exceed a minimum height of about 1 m in order to support heavy equipment. Additional criteria for 1.8 m height were not specified [*U.S. Army Corps of Engineers*, 2010a]. It was estimated that more than 8×10^6 m^3 of sand would be necessary for construction. At the proposed length and volume, this sand berm would exceed all prior coastal construction efforts in Louisiana [*Louisiana Department of Natural Resources*, 2013]. A major challenge to the construction effort was locating enough suitable sand in an otherwise muddy Mississippi River delta plain. The initial solution was to dredge sediment from a trench located 1 km offshore. Due to concerns about its proximity to the barrier island platform, the alternate site located just offshore of the island (Figure 4) was abandoned and in-filled with sediment from the main borrow site. Subsequently, it was determined that obtaining sand from an offshore trench was not practical and could be damaging to the island's integrity. Instead, sediment was pumped 4.5 km south to the berm from a single location seaward of Hewes Point. Dredging from this location could provide higher quality sediment, and was believed to be less likely to destabilize the island platform [*Lavoie et al.*, 2010].

©2014. American Geophysical Union. All Rights Reserved.

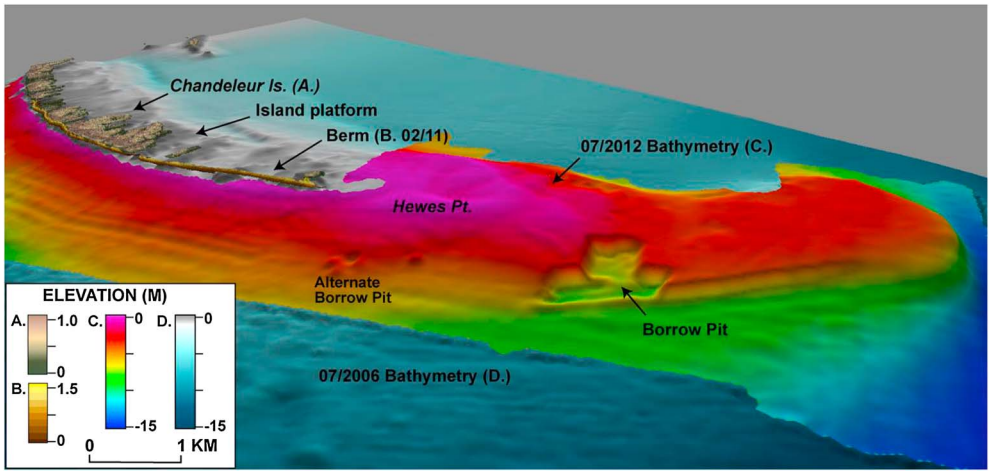

Figure 4. Perspective image of the Chandeleur Islands, berm, and surrounding seafloor. The image is a compilation of various data sets collected by the USGS including lidar topography of the islands (2007) and the berm (2011), swath and single beam bathymetry of the surrounding waters (2006) and of Hewes Point and nearshore (2012).

Construction of the berm (Figure 2) began in June 2010 and continued through April 2011 (Figure 3), long after the oil well had been capped in July 2010 and after observations of surface oil within the Gulf had ceased in August 2010. Only the first section (known as E-4) of the originally proposed trio of berms was completed. From north to south, the berm extended along the submerged apex of the island platform for approximately 8 km and then joined the island shoreface for an additional 4 km (Figure 3). Moving the berm onto the shoreface was necessary to reduce the required sand volume, construction cost, and increase the rate of construction [*U.S. Army Corps of Engineers*, 2010b]. As can be seen in the images that document the berm construction and evolution (Figure 3), the berm began to evolve due to processes such as overwash, breaching, and other forms of alongshore and cross-shore sediment transport divergence. These changes resulted from a wide range of conditions including winter and tropical storms.

Comparison of pre and postconstruction bathymetric surveys (Figure 4) revealed a 1.5 km^2 borrow area that was up to 4 m deep and we estimated had produced 3.5×10^6 m^3 of sediment. Construction volumes submitted to the U.S. Army Corps of Engineers estimate 4.1×10^6 m^3 of sediment was used to construct the berm, with 0.5×10^6 m^3 mined from an alternate borrow site [*Shaw Corporation*, 2011]. The volume of material used in construction amounts to roughly 4 years of deposition at Hewes Point and 2 years of natural shoreface erosion, based on averaged deposition over the past century [*Twichell et al.*, 2009]. Sediment transport estimates numerically estimated by *Ellis and Stone* [2006] yield much slower alongshore transport rates suggesting that the berm sediment would be redistributed to Hewes Point in about 50 years. However, since only fair-weather conditions were included in that study we suggest that 2–4 years, which includes a long-term average of all fair-weather and storm conditions, provides a better estimate of the sediment response time. Thus, if conditions at the Chandeleur Islands were to remain as they did over the past century, the berm would, on average, contribute approximately 1.0×10^6 m^3 of material to the island platform and return 1.5×10^6 m^3 to Hewes Point within 4 years. The balance of material (1.0×10^6 m^3) could remain in the shoreface, or be lost from the system.

3. Methods

3.1. Observations of Berm Evolution

The evolution of the Chandeleur berm was documented using airborne photographic and lidar surveys as well as interpretation of satellite imagery. While we have coverage of the berm and island evolution over a time span beginning prior to the Deepwater Horizon oil spill and spanning the entire lateral extent of the Chandeleur Islands and the berm, we have focused this analysis on the middle section of the berm which was built in front of the existing island (Figure 1), as opposed to the sections built on the submerged platform to the north or built directly on the shoreline to the south. Our analysis period began when the middle section of the berm was completed, as observed on 17 November 2010, and the analysis period ended when the berm disappeared after Tropical Storm Lee made landfall on 3 September 2011 (observed on 6 September 2011).

©2014. American Geophysical Union. All Rights Reserved.

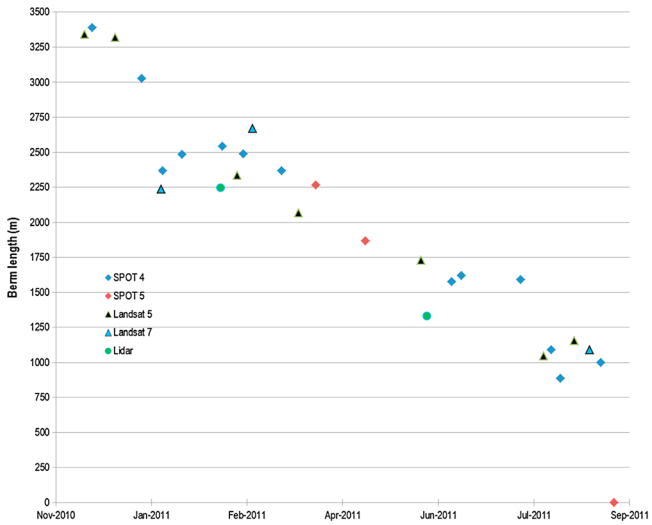

Figure 5. Berm length time series estimated from satellites (SPOT and Landsat) and lidar.

Satellite imagery was updated frequently (approximately every 7 days) and resolved the linear extent and position of the berm. Lidar observations were less frequent and were used as a secondary data source, primarily to evaluate the accuracy of the image-based observations since lidar data provide higher spatial resolution (about 1 m point spacing).

Details of the satellite and lidar analysis can be found in *Plant and Guy* [2013] and are described only briefly here. Satellite images from Landsat 5 (multispectral sensor with 30 m spatial resolution) and Landsat 7 (multispectral sensor with 30 m resolution, panchromatic sensor with 15 m resolution), SPOT 4 (multispectral with 20 m resolution, panchromatic with 10 m resolution), and SPOT 5 (multispectral with 10 m resolution, panchromatic with 5 m resolution) were utilized when they had a clear view of the berm. When available, the higher-resolution panchromatic bands were used instead of multispectral bands. When panchromatic bands were not available, single bands from the multispectral images were used. The satellite images were analyzed by a threshold-contouring method, wherein image intensities near the berm were contoured and then a particular contour was selected by a human analyst to identify the berm's footprint. This approach adapted to the variations in the lighting and image quality and produced a consistent set of berm outlines. The berm outlines were manually digitized to obtain the discontinuous length of berm remaining at each time. When the berm became fragmented, the total length of all the fragments was summed. Only berm footprints that overlapped with the original (i.e., as-built) footprint were included. Hence, length changes include direct changes in linear extent (e.g., in a berm following coordinate frame) as well as apparent changes due to cross-shore migration. We estimated the root-mean-square (rms) errors associated with individual berm length measurements to be about 250 m, based on comparing sequential pairs of images during times of minimal change. Comparison of berm length variations to water level variations showed no apparent correlation. The observations showed both increases and decreases in berm length (Figure 5) through time. Length changes included a general decreasing trend marked by two very large decreases after winter storms in late December 2010 and early January 2011 and after Tropical Storm Lee in September 2011. (After Lee, the berm length was zero.) Berm length increases may have resulted from littoral processes elongating the berm deposits, deposition of sand into recent breaches.

Six lidar surveys were conducted by the USGS as part of ongoing research efforts at the Chandeleur Islands. Lidar surveys (Figure 6) indicated absolute changes in elevation, but were not sampled frequently enough to resolve the timing of significant changes in both berm construction (apparent between March 2010 and June 2011) and berm degradation (apparent between February 2011 and September 2011). The lidar data indicated that the berm became narrower and lower, and migrated landward. The image-based length estimates are longer (by about 250 m) than the lidar-based estimates, likely due to differences in the reference elevation (1 m for lidar, unknown for imagery) used to define the berm outlines. However, based on the only two lidar surveys that fell within the study period, the longer-term trends of the berm length changes are very similar between the two data types.

3.2. Overwash Estimation

Our approach to predicting berm evolution assumed that berm overwash was the primary driver of rapid evolution, and that more gradual evolution resulted when overwash did not occur or was infrequent. Overwash occurred when the combination of tides, storm surges, and wave-induced water levels (i.e., wave setup and swash excursions, which are collectively called runup) exceeded the berm height [*Sallenger*, 2000; *Stockdon et al.*,

©2014. American Geophysical Union. All Rights Reserved.

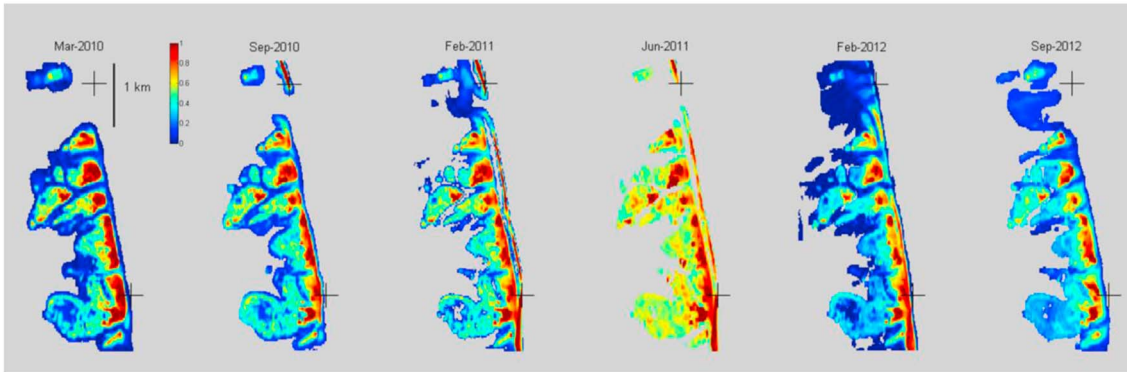

Figure 6. Lidar elevation time series. The black fiducial marks indicate the extent of the berm that was included in this analysis.

2006; *Stockdon et al.*, 2007; *Stockdon et al.*, 2009]. We developed a probabilistic model that estimated the runup components and returns a prediction of the likelihood of exceeding a particular berm elevation threshold:

$$p(R > Z) = \text{funct}\left(\vec{\eta}[x,y], \vec{H}[x,y], \vec{W}[x,y], \beta\right), \tag{1}$$

where R represents the runup elevation, Z is the berm elevation threshold, β is the berm face slope, and $\left(\vec{\eta}\ \vec{H}\ \vec{W}\right)$ represent the multidimensional characterization of water level (i.e., tide and surge), waves (height, period, and direction), and wind (speed and direction), respectively. To characterize the runup, we used Monte Carlo simulations of the formulation developed by *Stockdon et al.* [2006]. This formulation is

$$R = \eta_{\text{tide}} + \eta_{\text{surge}} + \eta_{\text{setup}} + \eta_{\text{swash}}, \tag{2a}$$

where $\eta_{\text{tide}} + \eta_{\text{surge}}$ are the observed or predicted nonwave water levels.

$$\eta_{\text{setup}} = 0.385\,\beta\sqrt{H_1 L_1} \pm e_{\text{setup}}, \tag{2b}$$

and

$$\eta_{\text{swash}} = N\left\{0, 0.412\,\beta\sqrt{H_1 L_1\left(1 + [0.0834/\beta]^2\right)} \pm e_{\text{swash}}\right\}. \tag{2c}$$

The two error terms ($e_{\text{setup}} = 0.21\ m, e_{\text{swash}} = 0.52\ m$) characterize the parameterization errors [*Stockdon et al.*, 2006]. These errors represent the mismatch between a large number of runup observations and the empirical model. The term H_1 is the significant wave height estimated near the 20 m contour (the subscript 1 signifies data at a location relevant to the berm) and L_1 is the deep-water wavelength of the waves reaching the berm and is a function of dominant wave period, T_1, ($L_1 = \frac{gT_1^2}{2\pi}$, where g is acceleration of

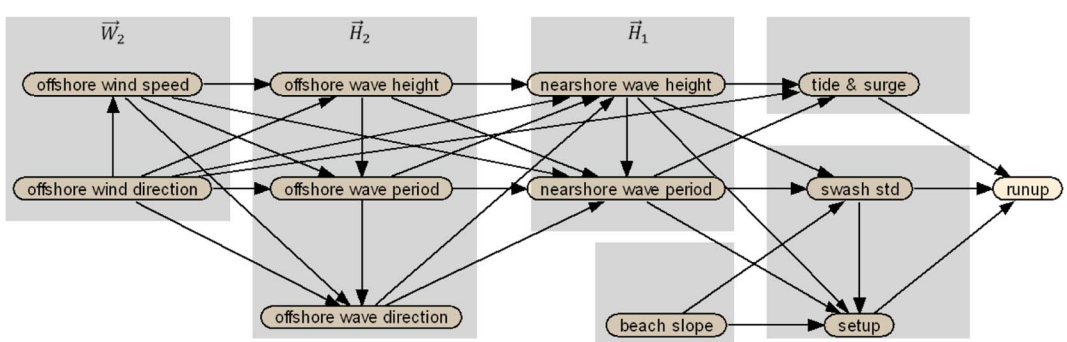

Figure 7. Schematic diagram of the Bayesian network used to predict runup levels at the berm. Each labeled element represents observed, modeled, or predicted variables. Each variable is allowed to take on a finite number of discrete states, and the arrows represent the conditional probabilities relating output variables to their inputs.

©2014. American Geophysical Union. All Rights Reserved.

gravity). The swash elevations are described by a normal distribution with the parameterized standard deviation (equation (2c)). Thus, runup combines water level variations that change both slowly (timescale of hours) and rapidly (seconds).

The parameterization described in equation (2) requires input wave height and period near the 20 m contour. Although NOAA gage 42007, in 15 m water depth, was located very near where we needed the input information (Figure 1), the buoy was removed prior to the berm construction. However, archival data existed and were used to develop a prediction based on more distant observations at gage 42040 in 160 m water depth (Figure 1). A probabilistic solution to equation (1) given the formulations in equation (2) and the additional wave modeling uncertainties was solved with a Bayesian network (Figure 7) and trained on the buoy observations and Monte Carlo runup simulations. The Bayesian network solves the problem stated in equation (1) as

$$p\left(R\middle|\vec{H}_2,\vec{W}_2\right) = p\left(\vec{H}_2,\vec{W}_2\middle|R\right)p(R)/p\left(\vec{H}_2,\vec{W}_2\right), \tag{3}$$

where the term $\vec{H}_2$ includes wave height, period, and direction and $\vec{W}_2$ includes wind speed and direction observed at the offshore location of buoy 42040 that must be transferred to location of buoy 42007. The term in the denominator of equation (3) represents the prior probabilities based on 15 years (1995–2009) of observations. The first term on the right-hand side of equation (3), $p\left(\vec{H}_2,\vec{W}_2\middle|R\right)$, is the likelihood of the observations given a particular value of runup. In practice, this is computed from (a) the estimated correlations between $\left(\vec{H}_2,\vec{W}_2\right)$ and $\left(\vec{H}_1\right)$ and water levels based on the synchronous observations (1995–2009) from the tide gage (Shell Beach tide station 8761305, Figure 1) and the two wave observation locations (buoys 42007 and 42040) and (b) correlations determined from Monte Carlo simulations of equation (2), with a beach slope constrained to the range 0.04 to 0.08, which is consistent with a value of 0.05 based on the initial lidar survey. About 70,000 runup calculations were included in the Monte Carlo simulations spanning different combinations of wave heights, periods, and beach slopes.

The Bayesian network discretized the values of the input and output variables into a finite number of states: wind and wave directions were divided into 30° increments; wind speed was divided into 10 increments with 2 to 5 m/s intervals; offshore wave height was divided into 9 increments with 1 to 5 m intervals; wave period was divided into 9 increments in 2 s intervals; tide level was divided into 10 increments with 0.5 to 1 m intervals; swash was divided into 8 increments with 0.25 m to 2 m intervals; setup was divided into 10 increments with 0.25 to 2 m intervals; and runup was divided into 24 increments with 0.25 to 5 m increments. The total number of combinations of all variables and all states yields 2,140,292 different scenarios (many of which are highly improbable) that span the range of conditions experienced at the study site. The efficacy of this approach has been demonstrated in other applications [*Plant and Holland*, 2011] for integrating observations and models and making accurate probabilistic predictions. The application of a Bayesian network solution to equation 3 is particularly appropriate here because it includes uncertainties in the observations at the deep location (42040), uncertainties in predicting values at the shallow location (42007), uncertainties in the actual beach slope, and uncertainties in the runup parameterization (equation (2)). These uncertainties were included in estimates of the probability that runup exceeded the berm elevation.

3.3. Berm Evolution

We assumed that the berm evolution between subsequent observations depended on the overwash intensity (i.e., the probability of overwash) as well as the duration of overwash events [*Donnelly et al.*, 2006]. Overwash probability can be estimated from buoy observations each hour and the number of hours of overwash occurring at a particular intensity can be used to account for overwash duration. For instance, a period with mild conditions will experience a long duration of low overwash probability. A period with a brief storm will have a long duration of low overwash probability and short durations of high overwash probability. A predictive equation that includes berm erosion due to both low overwash probability conditions (e.g., gradual changes not related to storms) and high overwash probability events and includes event duration is

$$y_i = \Delta t\left(b_0 + b_1\sum_i \delta_j\right), \tag{4}$$

where Δy_i is the change in berm length during the ith time period, $\delta_j = 1$ if $p_j > p^*$ and is 0 otherwise; p^* is a probability threshold defining high probability overwash events (e.g., $p^* = 1.5\%$ or 2%); Δt is an integration

©2014. American Geophysical Union. All Rights Reserved.

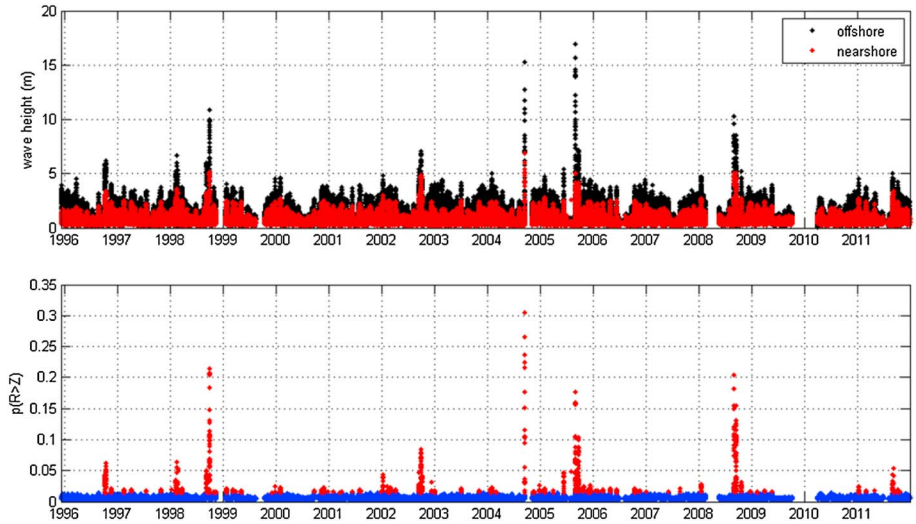

Figure 8. (top) Offshore wave height observations and nearshore wave height predicted from the Bayesian model. (bottom) Overwash predictions from the Bayesian model. Overwash probabilities exceeding 1.5% are marked with red dots.

interval, and j indicates the set of overwash prediction times within the integration period such that $t_{i-1} < t_j < t_i$. In equation (4), summing the contributions, δ_j, over each of the j hydrodynamic predictions (i.e., based on hourly buoy data) yields the modeled contribution to the less frequently sampled morphologic changes. The coefficients weight the influence of persistent conditions (b_0) and overwash events (b_1) on berm length changes when there are different numbers of events associated with the set of morphologic changes. Using the observed morphologic response data and predicted overwash probabilities, we determine the cumulative duration of events that exceeded p^* and then use the observed berm length change history to estimate the best fit model coefficients b_0,b_1, and p^*. The best fit model can be applied retrospectively to the historic record to investigate climatological variability in potential berm erosion events in order to determine whether the observed berm evolution was representative or anomalous in a climatological sense.

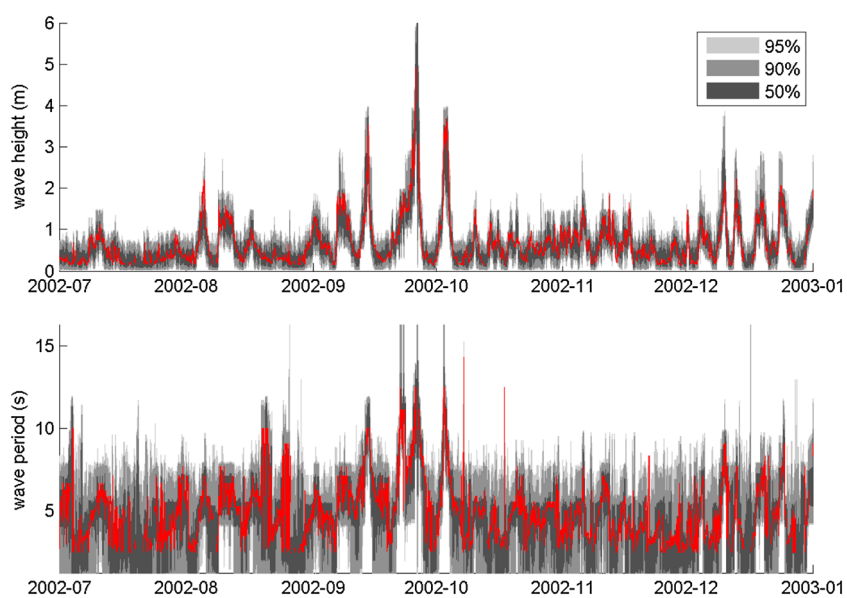

Figure 9. Bayesian network prediction (shaded confidence regions) of (top) wave height and (bottom) period at the nearshore location (42007, observations shown in red).

©2014. American Geophysical Union. All Rights Reserved.

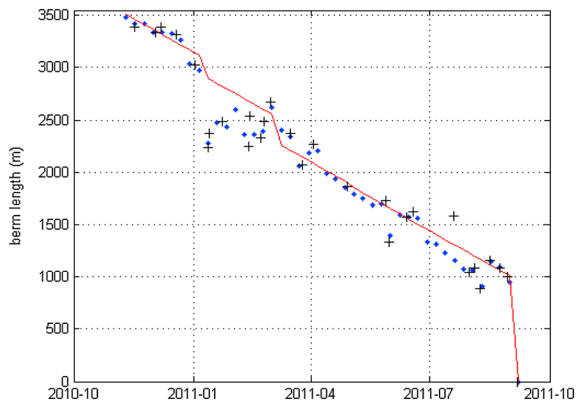

Figure 10. Prediction of berm length change (red line) including a constant rate term and an overwash exceedance term. The model was fit to berm lengths changes every 7 days (blue asterisk), which filtered some of the noise from the observations (black cross).

4. Results

4.1. Runup Predictions

Using observed wind and wave conditions at gage 42040, the Bayesian network was used to predict the probability of runup levels at the berm. The probabilities were then integrated over the range $R > 2$ m to determine overwash probabilities at each hourly observation interval. Figure 8 presents the time series of the offshore wave height used to force the Bayesian network model and the predicted nearshore wave height used to drive the runup component in the Bayesian network. Measured hourly wave period and direction, and wind speed and direction, were used as input. Water levels were not available for the entire period, so, for consistency, a level of 0.25 m with a large error (standard deviation of 0.5 m) was used to span the entire time period, allowing the Bayesian network to update the water level based on calculated correlations to winds and waves. A number of events appear in both the wave height observations and the overwash predictions (Figure 8). These include hurricanes Georges (in 1998), Lili (2002), Ivan (2004), Katrina (2005), and Ike (2008). In the period 2010–2012, tropical storm Lee is apparent in late 2011 and the overwash probability exceeded 5%. Otherwise, there are a number of smaller events such as winter storms that appear in the early part of each year. For the period affecting the berm evolution, there were three winter storm events in the early part of 2011.

The shallow-water significant wave height and peak period used for the *Stockdon et al.* [2006] runup parameterization is not required as an additional output from the Bayesian network since these predictions and their uncertainties are passed through the network directly to the runup prediction. It was, however, possible to assess the hindcast prediction skill of the shallow-water wave height during the period when gage 42007 was still operating. A sample comparison between the observations and the Bayesian network prediction of wave height (Figure 9, top) shows very good skill ($R^2 = 0.7$, mean error = 0.02 m, rms error = 0.25 m). Likewise, the wave period (Figure 9, bottom) prediction was also skillful ($R^2 = 0.9$, mean error = 0.07 s, rms error = 1.6 s). Because the Bayesian network predicts the probability of each wave height and period combination, the uncertainty of the prediction of these intermediate variables, and including their joint correlation, is passed on to the runup prediction and its uncertainty estimate.

4.2. Berm Length Change Predictions

The berm length changes were compared to the predicted overwash probabilities by interpolating the berm length data to smoothed observations at 7 day intervals and differencing these values in time. The cumulative number of events exceeding a probability threshold (e.g., p^*) that indicates overwash was counted for each 7 day interval. Previously, a probability threshold of 2% had been used to assess the likelihood of overwash extreme erosion [*Stockdon et al.*, 2007]. The reason that such low probabilities are meaningful is that if just 2% of the waves are capable of overtopping a berm, it is nearly certain that at least one wave in an hour (assuming 7 s period) would reach this level, and, for example, there is a 45% probability that ten waves could reach this level in an hour. We tried several probability thresholds in the application of equation (4) and found that storm events with predicted $p(R > Z) > 1.5\%$ were associated with berm breaching and large decreases in berm length. Presumably the threshold elevation required to drive berm erosion would decrease through time as the berm elevation was reduced. The role of berm elevation changes is explored in the discussion.

The berm length change model (equation (4)) was fit to the data (Figure 10) to determine the coefficient that predicted the rate of persistent erosion ($b_0 = 1$ m/d in this case) plus the coefficient that predicts changes due to overwash events ($b_1 = 50$ m/d for each day of overwash exceeding the p^* threshold). The model predicted an average berm length change rate that equaled the observed rate (11 m/d). The skill of the model fit to the berm length changes was 0.58, and the rms mismatch between the predicted and observed change rates was

©2014. American Geophysical Union. All Rights Reserved.

20 m/d. The model coefficients were statistically significant at the 95% confidence level. Results using probability thresholds of 1% or 2% were similar to those obtained using the 1.5% threshold. Use of the 1% threshold identified more events and the 2% threshold identified fewer events. Using the 1.5% threshold identified just four events, one each in January, March, April (barely visible in Figure 10), and September. The changes associated with below-threshold conditions, presumably driven by cross-shore, alongshore transport, and perhaps some minor overwash, but not associated with major overwash, are accounted for by the constant berm length decay term.

5. Discussion

We have developed and assessed probabilistic estimates of nearshore wave conditions that are passed to a well-calibrated runup parameterization [e.g., *Stockdon et al*., 2006] that is embedded via Monte Carlo simulation in a Bayesian network. The uncertainty in predicting wave conditions and runup elevations was propagated through the Bayesian network such that overwash probabilities included both the random nature of individual waves encountered over the nominally 1 h observation periods and our uncertainty in characterizing the random wave and runup statistics. The objective was to use these hydrodynamic predictions to predict the timing and magnitude of morphologic evolution of, in this case, the changing length of an engineered berm. The runup prediction was coupled to a morphodynamic response prediction by identifying an overwash probability threshold associated with relatively rapid erosion and adding this contribution to a term describing gradual evolution of berm length changes over the study period.

The Chandeleur berm provided a morphologic case study of a rapidly changing morphologic feature. More generally, our approach provides a robust, probabilistic assessment of the likelihood of significant coastal evolution based on assimilation of oceanographic and morphologic data. This approach can be implemented in near real time (i.e., updated each hour) and used for rapid response. For instance, we have already utilized this capability in scheduling the lidar and photography missions that collected the data used in this analysis to focus these missions on times when significant changes were likely to occur or had occurred. The predicted hindcast, nowcast, and forecast guidance served us well even before we had established its quantitative skill. Additionally, this capability can be used to evaluate "what-if" scenarios that are relevant to both engineered berm design and climate-change studies on natural or engineered features. For instance, what is expected if we utilized different storm climatology? Or, what if the berm elevation were changed? We explore these questions in the following sections.

5.1. Sensitivity to Climate Variability

Using our probabilistic model for predicting overwash events and subsequent berm evolution, we can determine the expected response of the berm (and, in principle, a broader range of barrier island morphologic features) had it existed at some other time in the past or future when the specific storm climatology may differ from the conditions observed during the life of this particular berm. This is directly relevant to establishing expectations for the performance of restoration features or the survival of natural barriers with and without climate change. The details of exactly how rapidly another feature evolves may depend on characteristics not captured here, such as feature width, sediment type, or sediment availability. But, examination of the occurrence of the number of events exceeding a threshold for rapid morphologic response (i.e., 1.5% overwash probability) should have broad applicability if we are interested in understanding the likelihood of significant evolution of a wide variety of barrier island features. Using the 1.5% threshold value for overwash probability, the number of events at this site that would have been likely to cause significant evolution of a 2 m high berm was computed and averaged over each year based on the offshore oceanographic inputs recorded over the period 1996 through 2012 (blue asterisks in Figure 11, top). The results are presented as the amount of time (days per year) that overwash probability exceeded the 1.5% threshold. This approach captured the overwash climatology over intra-annual through decadal time scales. Studies of past and future berm response can be based on the range of conditions that we have sampled or simulated oceanographic climatologies [e.g., *Bender et al*., 2010] could be used instead.

Over the observation period (1996–2012), the average overwash event-days per year ranged from a minimum of 1 to a maximum of 8 days, with an average 4 event-days per year. The years with many event-days include those with major hurricanes (e.g., Katrina and Rita in 2005). The mild years include 2010, the first year

©2014. American Geophysical Union. All Rights Reserved.

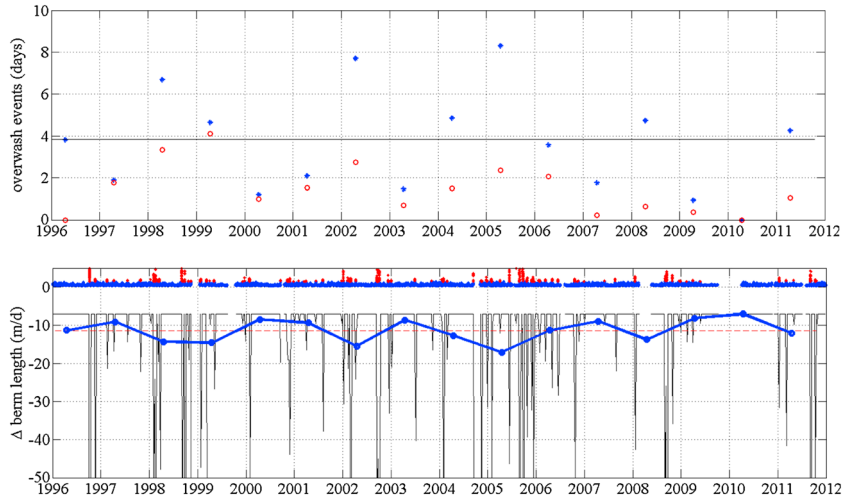

Figure 11. (top) Variation in cumulative overwash event days per year, including all months (blue asterisk) and the winter months (red open circles). Winter was defined as November through April. (bottom) Predicted berm length change for each 7 day time interval (black line) and averaged for each year (heavy blue line) from 1995 to present. The 1996–2012 average rate is shown with a red dashed line. The overwash probability shown in Figure 8 used to drive the predictions is repeated in Figure 11 (inset).

of the berm's existence. There were no events detected in 2010, partly due to missing wave data during the winter season. Over the life of the Chandeleur berm, there were about 4 event-days per year, which is very close to the expected long-term average. The events can be further subdivided by season in order to determine whether the overwash was due to tropical storms or winter cold fronts (Figure 11a; red circles mark events in the winter months of November through April). On average, 1.5 event-days occurred during the winter months. The number of overwash events in the first winter of the berm's existence (2011) was close to the average winter value.

Using the berm length evolution model, the overwash climatology can be transformed to give predicted berm length changes in each year (Figure 11, bottom). These predictions can be interpreted as giving the expected rate of berm decay if the berm had been subjected to storm climatologies other than that experienced in 2010 and 2011. Berm length changes were predicted for each 7 day period, and then these predictions were averaged for each year from 1996 to 2012. The largest annual berm length change rate was −17 m/d in 2005, the year of Hurricane Katrina, and the minimum annual change rate was −7 m/d in 2010. The long-term average, including both the gradual and event-driven change rates was −11 m/d. Thus, on average (as in 2010–2011), a 3.5 km berm could be expected to last about 10 months. During a year with mild storminess the berm could last a half year longer, and it might last just 6 months during a stormy year. These rates are relevant to overall barrier island evolution because they indicate how quickly sediment might be transferred from the berm to the island system. The potential sediment transfer from the berm can be compared to other sediment transport rates, such as the estimates from long-term volume change or models that predict island evolution in the absence of a berm. And, comparing the lidar elevation changes between March 2010 and September 2012 (Figure 6), suggests that there are not major increases in subaerial extent or elevation (in fact, decreases in both are apparent), and that if the berm sediment is still in the system it must be in the subaqueous portion of the island platform.

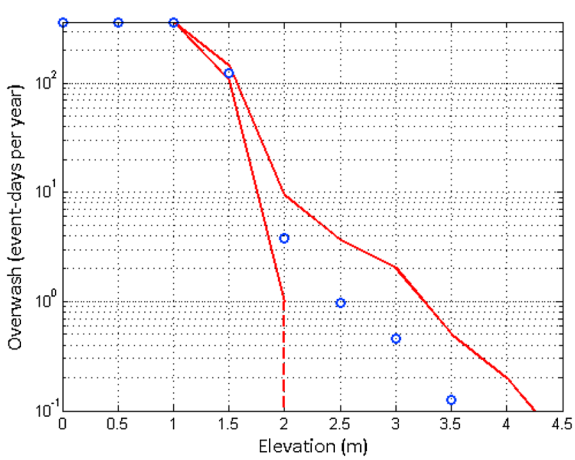

Figure 12. Summary of climate variability indicating average overwash event days per year (blue open circles) and extremes (red lines). The dashed red line indicates cases where a minimum of zero event days were observed at elevations of 2.5 m or higher.

©2014. American Geophysical Union. All Rights Reserved.

5.2. Sensitivity to Elevation Variability

Changes in berm elevation were not explicitly included in the analysis presented so far, where, instead, we focused on a constant elevation threshold for the purpose of consistency in comparing the impact of overwash events through time. However, we can examine the dependence of overwash on any elevation threshold, indicating sensitivity of the model to the assumption of static elevation as well describing the response that would be expected from different berm elevation designs or to analysis of the vulnerability of existing barrier islands [*Stockdon et al*., 2012]. Using the output of the runup probability from the Bayesian model, we extracted exceedence probabilities for elevation thresholds ranging from 0 to 4.5 m in 0.5 m increments. For each elevation threshold, we extracted the number of event-days ($p(R > Z) > 1.5\%$) per year over the 1996 to 2012 period and computed the average, minimum, and maximum values for all years (Figure 12).

The sensitivity of the number of overwash events to the threshold elevation is low at very low elevations. For elevations less than 1 m, it is likely that small waves and changes in water level could produce an overwash event every day. Between 1.5 and 2 m elevation, the overwash probability is sensitive to changes in elevation (i.e., the slope of the curve is steep in Figure 12). The overwash likelihood decreases with increasing elevation over 2 m, and overwash likelihood is reduced by an order of magnitude to an average of 0.1 event-days per year (i.e., one event-day per decade) at a threshold elevation of 3.5 m. At this elevation, the maximum response is 0.5 event-days per year, or 20 times fewer events than for a 2 m high berm, and the minimum response is zero event-days in a year, which is also the minimum for all elevations greater than 2 m.

5.3. Alternative Approaches

There are a number of alternative approaches that could have been employed to provide a similar prediction capability and assessment of barrier island climatological and elevation sensitivities. For instance, we could have used a detailed wave-evolution model that is implemented on a high-resolution spatial grid and solves equations for mass and momentum fluxes and conservation, such as Simulating Waves Nearshore [e.g., *Booij et al*., 1999; *Ris et al*., 1999] or WaveWatch models to provide inputs to the runup model. There are numerous examples where this has been done already for the Chandeleur Islands [*Ellis and Stone*, 2006; *Interagency Performance Evaluation Task Force* (*IPET*), 2007; *Lindemer et al*., 2010; *Stockdon et al*., 2012]. One drawback to using a more detailed modeling approach is that the numerical model outputs do not intrinsically characterize prediction uncertainties that may stem from errors in boundary condition data or bathymetry, or poorly constrained model parameters [*Apotsos et al*., 2008]. Also, more detailed models are computationally expensive when simulating long time periods, and the expense often includes wasteful repetition of time periods with virtually identical wave properties. The Bayesian network's skill suggests that the observed record sufficiently sampled most conditions, even infrequent hurricanes, to adequately represent the likelihood of exceeding overwash thresholds. The main drawback with the Bayesian approach is that the present implementation is trained to reproduce predictions at very specific locations (e.g., buoys 42040 and 42007) and must be retrained for applications to other locations. However, there are plenty of data or model simulations available for training at nearly any coastal location.

Likewise, a deterministic numerical simulation of morphological change using models such as Delft-3D [*Lesser et al*., 2004] or Xbeach [*Roelvink et al*., 2009] could be conducted using the same or more detailed oceanographic inputs as employed here. Examples of skillful predictions during storm conditions are increasingly numerous [*Roelvink et al*., 2009; *Lindemer et al*., 2010; *Mccall et al*., 2010]. But, there is little evidence that these very detailed models, which resolve the 2-D or 3-D wave, flow, and sediment transport fields, can simultaneously predict storm events and the intervening moderate conditions. For longer-term applications, approaches that rely on some fitting of the models to morphological data appear to be required to maintain skill. The class of data-fitting statistical models, such as were employed in the present approach, have been applied to prediction of specific morphologic or topographic features, including the shoreline [*Yates et al*., 2009; *Long and Plant*, 2012] and sandbars [*Plant et al*., 1999; *Pape et al*., 2010; *Splinter et al*., 2011]. Thus, at the moment, accurate prediction of morphologic evolution appears to require some element of model-data assimilation. These applications require measured initial values of the morphology and some morphological updates. These updates could, for example, be obtained from lidar-derived beach and dune metrics [e.g., *Stockdon et al*., 2009 and many others; *Stockdon et al*., 2012] that include horizontal or vertical characteristics. Horizontal characteristics, such as the length observations that were extracted from satellite imagery used in this study, are readily available at all coastal locations. Oceanographic boundary conditions are also required

©2014. American Geophysical Union. All Rights Reserved.

to drive modeled response and can be obtained from either observations (as in our case) or large-scale climate, wave, and flow models. And prior data sets of the morphologic change are required to constrain free model parameters. These requirements can be met using the same modern observing and modeling capabilities that are used to initialize and drive the predictions. Finally, the assimilation and prediction capabilities of the Bayesian approach are particularly appropriate when prediction uncertainties from a broad range of sources and time scales must be considered, whether due to modeling limitations or unknown future climates. These uncertainties are clearly relevant to studies of barrier island evolution, protection, and restoration.

6. Conclusions

It is well known that overwash drives significant evolution of barrier islands and associated dunes and shoreline, including a wide variety of natural or restored settings. We have shown that this is true for smaller features such as berms. We have extended a probabilistic approach to predict overwash by coupling overwash predictions to berm length change predictions. The inputs to the overwash prediction were nearshore wave conditions, which, in turn, were predicted from observed data obtained from a buoy relatively far from the location of interest. The intermediate nearshore wave predictions were compared to historic wave data and the model was shown to have good prediction skill ($R^2 = 0.7$ and 0.9 for wave height and period, respectively). Data were not available to independently test the overwash predictions, and the evaluation of overwash prediction skill was necessarily confounded with the assessment of berm length prediction skill. Using lidar topography and satellite imagery, we have demonstrated that the evolution of a sand berm constructed near the Chandeleur Islands was predicted well from a simple model that accounts for overwash intensity (i.e., probability of overwash) and duration (measured as the amount of time that overwash at a predicted intensity has occurred) along with gradual berm erosion due to nonoverwash processes. This approach captured the erosion of the sand berm as quantified by changes in alongshore length.

Our berm length modeling approach required fitting two free parameters to give the best prediction of berm length changes. The predictions were then generalized to provide broader insight and guidance for determining the rate of overwash-driven erosion of both natural and man-made features along barrier island coastlines with different climatologies and different feature elevations. The inputs required for broad application of our approach include wave and water level climatologies, which could be obtained from observations, deterministic models, probabilistic models, or some combination of observations and models as was done here. The output is a systematic analysis of overwash and erosion events as a function of storminess (i.e., years with mild versus severe storms) and feature elevation. As has been shown by others, systematic prediction of overwash is an excellent indicator of morphologic change, particularly for features that lack vigorous regeneration mechanisms, such as low berms, transgressive submergence shorelines, and even some dunes. In our case, based on the climate record and parameterized runup predictions, a 2 m high berm built in front of the Chandeleur Islands was expected to overwash at least 1 day per year, and, on average, a total of 4 days each year. During the period spanned by our morphologic observations, the actual berm overwash rate was 4.25 days per year, which was nearly the same as the long-term average. Additional analysis of the elevation dependence of overwash in the context of the storminess climatology showed that a berm constructed at 3.5 m height would be much less likely to experience overwash, with an average of only a single overwash event-day per decade. Understanding these rates of overwash and related morphologic change ultimately improves our understanding of the interaction between barrier islands and berms (or other perturbations, including a variety of restoration projects) and the storminess associated with future climates.

Acknowledgments
This research was initiated by the construction of the emergency sand berm which had a cost of several hundred million dollars. We thank Amar Nayegandhi who honed our approach to planning, collecting, and analyzing lidar data, Chris Sherwood who galvanized the original effort to build a research project around the berm, and Abby Sallenger. Abby's contribution went beyond the specifics of this particular project and included many conversations about the role of our research and its impact on society. Abby died 5 February 2013. We thank Guy Gelfenbaum, Laura Moore, and two anonymous reviewers, as well as JGR-ES Editor and Associate Editor for providing constructive comments that greatly improved the final manuscript.

References

Anderson, T. R., N. L. Frazer, and C. H. Fletcher (2010), Transient and persistent shoreline change from a storm, *Geophys. Res. Lett.*, *37*, L08401, doi:10.1029/2009GL042252.

Apotsos, A., B. Raubenheimer, S. Elgar, and R. T. Guza (2008), Testing and calibrating parametric wave transformation models on natural beaches, *Coastal Eng.*, *55*, 224–235.

Bender, M. A., T. R. Knutson, R. E. Tuleya, J. J. Sirutis, G. A. Vecchi, S. T. Garner, and I. M. Held (2010), Modeled impact of anthropogenic warming on the frequency of intense Atlantic hurricanes, *Science*, *327*, 454.

Booij, N., R. C. Ris, and L. H. Holthuijsen (1999), A third generation wave model for coastal region: 1. Model description and validation, *J. Geophys. Res.*, *104*(c4), 7649–7666.

Cattaneo, A., and R. J. Steel (2003), Transgressive deposits: A review of their variability, *Earth Sci. Rev.*, *62*(3–4), 187–228.

Donnelly, C., N. Kraus, and M. Larson (2006), State of knowledge on measurement and modeling of coastal overwash, *J. Coast. Res.*, *22*(4), 965–991.

©2014. American Geophysical Union. All Rights Reserved.

Ellis, J., and G. W. Stone (2006), Numerical simulation of net longshore sediment transport and granulometry of surficial sediments along Chandeleur Island, Louisiana, USA, *Mar. Geol.*, *232*, 115–129.

Fearnley, S. M., M. D. Miner, M. Kulp, C. Bohling, and S. Penland (2009), Hurricane impact and recovery shoreline change analysis of the Chandeleur Islands, Louisiana, USA: 1855 to 2005, *Geo-Mar. Lett.*, *29*, 455–466.

Flocks, J., D. Twichell, J. Sanford, E. Pendleton, and W. Baldwin (2009), Chapter f. Sediment sampling analysis to define quality of sand resources, in *Sand Resources, Regional Geology, and Coastal Processes of the Chandeleur Islands Coastal System—An Evaluation of the Breton National Wildlife Refuge*, edited by D. Lavoie, *U.S. Geol. Surv. Scientific Investigations Rep. 2009–5252*, pp. 99–124.

Froede, C. R., Jr. (2008), Changes to Dauphin Island, Alabama, brought about by Hurricane Katrina (August 29, 2005), *J. Coast. Res.*, *24*(4c), 110–117.

Interagency Performance Evaluation Task Force (IPET) (2007), Performance evaluation of the New Orleans and Southeast Louisiana Hurricane Protection System, in *Final Report of the Interagency Performance Evaluation Task Force*, 282 pp., US Army Corps of Engineers, Washington, D. C.

Jackson, N. L., K. F. Nordstrom, R. A. Feagin, and W. K. Smith (2013), Coastal geomorphology and restoration, *Geomorphology*, *199*, 1–7.

Kelley, J. T. (2013), Popham Beach, Maine: An example of engineering activity that saved beach property without harming the beach, *Geomorphology*, *199*, 171–178.

Kroonenberg, S. B., E. N. Badyukova, J. E. A. Storms, E. I. Ignatov, and N. S. Kasimov (2000), A full sea-level cycle in 65 years: Barrier dynamics along Caspian shores, *Sediment. Geol.*, *134*(3–4), 257–274.

Lavoie, D., J. G. Flocks, J. L. Kindinger, A. H. Sallenger Jr., and D. C. Twichell (2010), Effects of building a sand barrier berm to mitigate the effects of the deepwater horizon oil spill on Louisiana marshes, *U.S. Geological Survey, Open-File Rep. 2010–1108*, 7 pp.

Lesser, G. R., J. A. Roelvink, J. A. T. M. van Kestera, and G. S. Stelling (2004), Development and validation of a three-dimensional morphological model, *Coastal Eng.*, *51*, 883–915.

Lindemer, C. A., N. G. Plant, J. A. Puleo, D. M. Thompson, and T. V. Wamsley (2010), Numerical simulation of a low-lying barrier island's morphological response to Hurricane Katrina, *Coastal Eng.*, *57*(11–12), 985–995.

Long, J. W., and N. G. Plant (2012), Extended Kalman Filter framework for forecasting shoreline evolution, *Geophys. Res. Lett.*, *39*, L13603, doi:10.1029/2012GL052180.

Louisiana Department of Natural Resources (2010), U.S. Army corps of engineers joint permit application for work within the Louisiana coastal zone, [Available at http://www.lacpra.org/assets/docs/Berm%20File/Berm%20Permit%20Application.pdf.]

Louisiana Department of Natural Resources (2013), Coastal use permit database, [Available at http://sonris.com/direct.asp?server=sonris-www&path=/sonris/cmdPermit.jsp?sid=PROD.]

McCall, R. T., J. S. M. de Vries Van Thiel, N. G. Plant, A. R. Van Dongeren, J. A. Roelvink, D. M. Thompson, and A. J. H. M. Reniers (2010), Two-dimensional time dependent hurricane overwash and erosion modeling at Santa Rosa Island, *Coastal Eng.*, *57*(7), 668–683.

Miner, M. D., M. Kulp, H. D. Weathers, and J. Flocks (2009), Historical (1869–2007) sea floor evolution and sediment dynamics along the Chandeleur Islands, in *Sand Resources, Regional Geology, and Coastal Processes of the Chandeleur Islands Coastal System—An Evaluation of the Breton National Wildlife Refuge*, edited by D. Lavoie, *U.S. Geol. Surv. Scientific Investigations Rep. 2009–5252*, pp. 47–74, U.S. Geological Survey, Reston.

National Aeronautics and Space Administration (2010), Earth observing satellite imagery (eo-1), [Available at http://earthobservatory.nasa.gov/NaturalHazards/view.php?id=43903.]

Pape, L., N. G. Plant, and B. G. Ruessink (2010), On cross-shore migration and equilibrium states of nearshore sandbars, *J. Geophys. Res.*, *115*, F03008, doi:10.1029/2009JF001501.

Penland, S., R. Boyd, and J. Suter (1988), Transgressive depositional systems of the Mississippi Delta plain: Model for barrier shoreline and shelf sand development, *J. Sediment. Petrol.*, *58*, 932–949.

Plant, N. G., and K. K. Guy (2013), Change in the length of the middle section of the Chandeleur Islands oil berm, November 17, 2010, through September 6, 2011, *U.S. Geological Survey Open-File Rep. 2013–1075*, 11 pp.

Plant, N. G., and K. T. Holland (2011), Prediction and assimilation of surf-zone processes using a Bayesian network. Part I: Forward models, *Coastal Eng.*, *58*(1), 119–130.

Plant, N. G., and H. F. Stockdon (2012), Probabilistic prediction of barrier-island response to hurricanes, *J. Geophys. Res.*, *117*, F03015, doi:10.1029/2011JF002326.

Plant, N. G., R. A. Holman, M. H. Freilich, and W. A. Birkemeier (1999), A simple model for interannual sandbar behavior, *J. Geophys. Res.*, *104*(C7), 15,755–15,776.

Price, W. A. (1951), Barrier Island, not "offshore bar", *Science*, *113*(2939), 487–488.

Riggs, S. R., D. V. Ames, S. J. Culver, D. J. Mallinson, D. R. Corbett, and J. P. Walsh (2009), Eye of a human hurricane: Pea Island, Oregon Inlet, and Bodie Island, northern Outer Banks, North Carolina, *in America's Most Vulnerable Coastal Communities*, Geological Society of America Special Paper 460-04, edited by J. T. Kelley, O. H. Pilkey, and J. A. G. Cooper, Geol. Soc. Am., Boulder, pp. 43-72, doi:10.1130/2009.2460(04).

Ris, R. C., L. H. Holthuijsen, and N. Booij (1999), A third generation wave model for coastal regions: 2. Verification, *J. Geophys. Res.*, *104*(c4), 7667–7681.

Roelvink, J. A., A. Reniers, A. V. Dogeren, J. V. T. de Vries, R. McCall, and J. Lescinski (2009), Modeling storm impacts on beaches, dunes and barrier islands, *Coastal Eng.*, *56*, 1133–1152.

Saalfeld, S. T., W. C. Conway, D. A. Haukos, and W. P. Johnson (2012), Snowy plover nest site selection, spatial patterning, and temperatures in the Southern High Plains of Texas, *J. Wildl. Manage.*, *76*(8), 1703–1711.

Sallenger, A. H., Jr. (2000), Storm impact scale for barrier islands, *J. Coast. Res.*, *16*(3), 890–895.

Schroeder, P. M., R. Dolan, and B. P. Hayden (1977), Vegetation changes associated with barrier-dune construction on the outer banks of North Carolina, *Environ. Manage.*, *1*(2), 105–114.

Schupp, C. A., N. T. Winn, T. L. Pearl, J. P. Kumer, T. J. B. Carruthers, and C. S. Zimmerman (2013), Restoration of overwash processes creates piping plover (Charadrius melodus) habitat on a barrier island (Assateague Island, Maryland), *Estuarine Coastal Shelf Sci.*, *116*, 11–20.

Shaw Corporation (2011), Construction presentation to the U.S. Army corps of engineers, April, 07, 2011.

Splinter, K. D., R. A. Holman, and N. G. Plant (2011), A behavior-oriented dynamic model for sandbar migration and 2DH evolution, *J. Geophys. Res.*, *116*, C01020, doi:10.1029/2010JC006382.

Stapor, F. W., Jr., and G. W. Stone (2004), A new depositional model for the buried 4000 yr bp New Orleans barrier: Implications for sea-level fluctuations and onshore transport from a nearshore shelf source, *Mar. Geol.*, *204*(1–2), 215–234.

Stockdon, H. F., R. A. Holman, P. A. Howd, and A. H. Sallenger Jr. (2006), Empirical parameterization of setup, swash, and runup, *Coastal Eng.*, *53*, 573–588.

Stockdon, H. F., A. H. Sallenger Jr., R. Holman, and P. Howd (2007), A simple model for the spatially-variable coastal response to hurricanes, *Mar. Geol.*, *238*, 1–20.

©2014. American Geophysical Union. All Rights Reserved.

Stockdon, H. F., K. S. Doran, and A. H. Sallenger Jr. (2009), Extraction of lidar-based dune-crest elevations for use in examining the vulnerability of beaches to inundation during hurricanes, *J. Coast. Res., Special Issue*, *53*, 59–65.

Stockdon, H. F., K. J. Doran, D. M. Thompson, K. L. Sopkin, N. G. Plant, and A. H. Sallenger (2012), National assessment of hurricane-induced coastal erosion hazards: Gulf of Mexico, *U.S. Geological Survey Open-File Rep. 2012–1084*, 51 pp.

Suter, J., S. Penland, S. J. Williams, and J. Kindinger (1988), Transgressive evolution of the Chandeleur Islands, Louisiana, *Trans. - Gulf Coast Assoc. Geol. Soc.*, *38*, 315–322.

Swift, D. J. P. (1975), Barrier-island genesis: Evidence from the central Atlantic shelf, eastern U.S.A, *Sediment. Geol.*, *14*(1), 1–43.

Tamura, T. (2012), Beach ridges and prograded beach deposits as palaeoenvironment records, *Earth Sci. Rev.*, *114*(3–4), 279–297.

Thompson, T. A., and S. J. Baedke (1995), Beach-ridge development in Lake Michigan: Shoreline behavior in response to quasi-periodic lake-level events, *Mar. Geol.*, *129*, 163–174.

Twichell, D., E. Pendleton, W. Baldwin, and J. Flocks (2009), Subsurface control on seafloor erosional processes offshore of the Chandeleur Islands, Louisiana, *Geo Mar. Lett.*, *29*(6), 349–358.

U.S. Army Corps of Engineers (2010a), Corps decision on state's emergency permit request, *News Release, 27 May 2010*.

U.S. Army Corps of Engineers (2010b), Permit modification request for reach e-4, special condition 19 amended to usfws special use permit 43556-10-01, October 4, 2010.

van den Hoek, R. E., M. Brugnach, and A. Y. Hoekstra (2012), Shifting to ecological engineering in flood management: Introducing new uncertainties in the development of a building with nature pilot project, *Environ. Sci. Policy*, *22*(0), 85–99.

Yates, M. L., R. T. Guza, and W. C. O'Reilly (2009), Equilibrium shoreline response: Observations and modeling, *J. Geophys. Res.*, *114*, C04014, doi:10.1029/2010JC006681.

©2014. American Geophysical Union. All Rights Reserved.